American Journal of Polymer Science and Technology
2016; 2(1): 1-10
http://www.sciencepublishinggroup.com/j/ajpst
doi: 10.11648/j.ajpst.20160201.11

Synthesis and Characterization of a High Oil-Absorbing Poly (Methyl Methacrylate-Butyl Acrylate)/ATP–Fe_3O_4 Magnetic Composite Material

Fathelrahman Mohammed Soliman[1, 2], Wu Yang[1], Hao Guo[1], Mahgoub Ibrahim Shinger[3], Ahmed Mahmoud Idris[3], Emtenan Suliman Hassan[4]

[1]Analytical Chemistry (Functional Materials), College of Chemistry and Chemical Engineering, Northwest Normal University, Lanzhou, China

[2]Key Lab of Eco-environment Related Polymer Materials of MOE, College of Chemistry and Chemical Engineering, Northwest Normal University, Lanzhou, China

[3]Analytical Chemistry (Photocatalysis), College of Chemistry and Chemical Engineering, Northwest Normal University, Lanzhou, china

[4]Analytical Chemistry (Functional Materials), College of Chemistry and Chemical Engineering, Northwest Normal University, Lanzhou, China

Email address:

fathy.19867@gmail.com (F. M. S), 1946003262@qq.com (F. M. S), 1946003262@qq.com (Wu Yang), 2479881695@qq.com (Hao Guo), Shinger1977@yahoo.com (M. I. Shinger), Ahmed63@163.com (A. M. Idris), 2856815011@qq.com (E. S. Hassan)

To cite this article:

Fathelrahman Mohammed Soliman, Wu Yang, Hao Guo, Mahgoub Ibrahim Shinger, Ahmed Mahmoud Idris, Emtenan Suliman Hassan. Synthesis and Characterization of a High Oil-Absorbing Poly (Methyl Methacrylate-Butyl Acrylate)/ATP–Fe_3O_4 Magnetic Composite Material. *American Journal of Polymer Science and Technology.* Vol. 2, No. 1, 2016, pp. 1-10. doi: 10.11648/j.ajpst.20160201.11

Received: July 10, 2016; **Accepted**: August 19, 2016; **Published**: August 30, 2016

Abstract: A highly oil-absorptive Poly (methyl methacrylate-butyl acrylate)/ ATP–Fe_3O_4 magnetic composite resin was prepared by a conventional suspension polymerization using methyl methacrylate, and butylacrylate were used as monomers, and N, N-methylenebis acrylamide (MBA) as crosslinking agent and ammonium persulfate (APS) as initiator on the modified ATP–Fe_3O_4substrate. The optimum reaction condition was examined in detail. The results indicated that the prepared composite resin combined characteristics of stronger magnetism and higher oil absorbency. The resultant resin had high oil absorbency and the highest absorbencies respectively reaches 23.8, 25, 30.0, 32.6g.g for xylene, toluene, carbon tetrachloride and chloroform, which were higher than some oil absorptive materials previously reported. At the same time, it could easily be recovered and reused too. Kinetic investigation proved that the oil absorption obeyed the pseudo-first-order kinetic model and intraparticle diffusion model.

Keywords: High Oil-Absorption, Magnetic Composite Resin, Modified ATP–Fe_3O_4

1. Introduction

Oil pollution of marine environments is becoming a serious issue with the growth of the off-shore petroleum industry and the necessity of marine oil transportation. Various Materials, including natural absorbents and synthesized polymeric materials, for example, brick clay, activated carbon, silicon dioxide, polyurethane foam, paper pulp, polypropylene fiber, and oil absorbing resin, have been employed to deal with oil pollution hazards and recover the spilled oils on water. Among them, the capability of oil-absorbing resin is seen to be superior to other ordinary materials [1-4]. High oil-absorption resin, different from ordinary oil-absorption material, is a new kind of self-swelling oil-absorbing material with many virtues of large absorbing quantity and variety of oils, as well as good oil-retention, and has a promising future. Synthesis and application of high oil-absorption resins have very important practical significance in environment protection and medicine, and so on. It is this broad range of possible

applications that has led to recent interest in this system [5, 6]. In previous work, the magnetite-covered clay particles were prepared with Na-montmorillonite flakes as supports [7]. Clays offer an option for the removal of organic and inorganic contaminants [8]. The adsorption of several organic contaminants in water such as pesticides, phenols, and chlorophenols has been widely reported recently [9–15]. The adsorption capacity of clays results from a relatively high surface area and a net negative charge on their structure. Attapulgite (ATP), one of these clays with the same functions but different structure, possessing of an ideal molecular formula of $[Si_8Mg_5O_{20}(OH)_2(H_2O)_4{\cdot}4H_2O$, is a kind of natural fibrous mineral, has also been widely used in polymer nanocomposite due to its large specific surface area, adjustable surface chemistry, non-toxicity, low cost and abundance in nature [16-19].

In this work, Poly (methyl methacrylate-butyl acrylate)/ATP–Fe_3O_4, magnetic composite resin with high oil-absorbency were synthesized by a suspension copolymerization on the modified ATP–Fe_3O_4 substrate. ATP-Fe_3O_4 magnetic particles, possessing special structure, stable properties and low-cost, were coated with a thin layer of poly (MMA-BA). Poly (MMA-BA) was obtained using methyl methacrylate and butylacrylate as monomers, and N, N-methylenebisacrylamide as crosslinking agent, ammonium persulfate (APS) as initiator, and gelatin as the dispersants. The influencing factors on the oil absorbency of the high-oil-absorption resin were studied in detail including the monomers mass ratio, amounts of the cross linking agent, initiator, and ATP–Fe_3O_4. The oil absorbency for several organic compounds (representative oil contaminations) was examined.

2. Experimental

2.1. Materials

Methyl methacrylate (MMA), butyl acrylate (BA) were washed with 5% sodium hydroxide three times before use, and then washed with deionized water until neutralization. After being dried over anhydrous magnesium sulfate, they were distilled twice under reduced pressure. N, N-methylenebisacrylamide (MBA) was used as received. Ammonium persulfate (APS) was recrystallized from water. Benzoyl peroxide (BPO) (Kang-Wei Chemical Reagent Factory, Shanghai, China). Attapulgite nano-fibrillar clay provided by Gansu ATP Co. Ltd., Gansu, China, was milled and passed through a 320-mesh screen before use. Ferric chloride hexahydrate ($FeCl_3.6H_2O$), ferrous chloride tetrahydrate ($FeCl_2.4H_2O$) and ammonium hydroxide (NH_4OH, 25% of ammonia), gelatin glue (Chemical Reagent Factory, Shanghai, China), toluene, xylene, carbon tetrachloride, and chloroform were of analytical reagent grade.

2.2. Synthesis of the ATP–Fe_3O_4 Magnetic Particles

The synthetic process of ATP–Fe_3O_4 magnetic particles was carried out by a modified co-precipitation method [17]. The ATP was dispersed into water and then pretreated with the $FeCl_3$ salt in flask under magnetic stirring as following: 4.0 g of $FeCl_3.6H_2O$ was added into water (total volume: 200 ml), then 1.50 g of attapulgite was dispersed into the above mixture in ultrasonic bath for 30 min to obtain a stable suspension. And last, the mixture was stirred for 12 h under magnetic stirring and the suspension was used for further experiments directly.

A given concentration of $FeCl_2$ solution was added to the suspension of ATP with $FeCl_3$ in N_2 atmosphere. After the solution was heated to 90°C, different amount of NH_4OH (25%, w/w) (6.0 ml, 3.0 ml, 2.0 ml, or 2.0 ml) was added rapidly under stirring and black precipitate appeared immediately. The mixture was kept under stirring for another 1 h. The products were precipitated and washed with water after the reaction mixtures were cooled to room temperature. Finally, the black product ATP–Fe_3O_4 magnetic particles were dried in the vacuum.

2.3. Preparation of the Composite Resin

A given amount of gelatin glue was dissolved in a known volume of distilled water in a 250-ml round bottomed flask equipped with stirrer and a reflux condenser at 30°C for 30 min. The mixture of butylacrylate, methyl methacrylate and MBA was then added to the above flask, as well as APS and modified ATP–Fe_3O_4. After suspension reaction for 6h at the stirring speed of 200 rpm under nitrogen atmosphere at 90°C, the prepared composite resin was collected by filtration when the solution was cooled, then washed with hot water of 60°C, and dried in a vacuum at 60°C until a constant weight was reached.

Synthesis and oil absorption of the magnetic high oil absorption resin field were shown in Fig. 1.

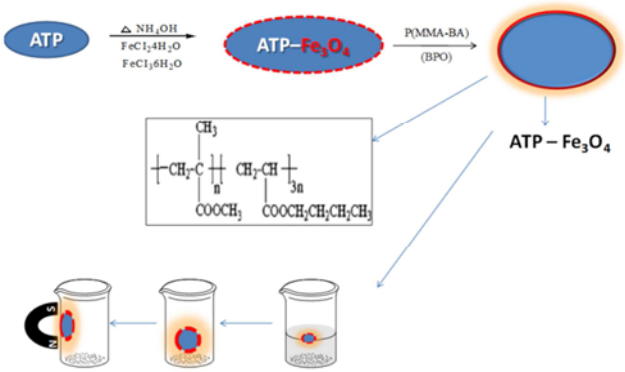

Fig. 1. *Synthesis and oil absorption operation of the magnetic high oil absorption resin.*

2.4. Characterization

2.4.1.Fourier Transforms Infrared (ATR FT-IR)

The attenuated total reflectance Fourier transform infrared (ATR FT-IR) spectra were collected by using a Nicolet NEXUS 670 FT-IR single-beam spectrometer (USA) with a 4 cm^{-1} resolution maintaining constant contact pressure between the Ge crystal and the specimens.

2.4.2.Thermogravimetric Analysis

Thermal stability measurements were performed on a Metter Toledo TG apparatus (Switzerland) from 30 to 800°C, with a heating rate of 10°C/min under a nitrogen flow rate of 50 mL/min.

2.4.3.Transmission Electron Microscopy (TEM)

The morphology and structure of the composite particles was determined by transmission electron microscopy (TEM) on a JEM 100 CX instrument (JEOL Co., Japan).

2.4.4. Scanning Electron Microscopy (SEM)

Scanning electron microscopy (SEM) images were taken with a JSM-5600LV scanning electron microscope (Japan) at an applied voltage of 20 kV.

2.4.5. X-ray Diffraction (XRD)

A crystallographic study was performed on the ATP-Fe_3O_4 modified by D/max 2400 X-ray diffractometer (XRD; Rigaku, Japan) by using Fe K and radiation. Magnetic properties were detected by vibrating sample magnetometer (VSM) (Lakeshore 7304).

2.4.6. Removal of Oil

The sample was immersed in various oils for given time periods at room temperature and then taken out from the oil. The excess oil on the resin surfaces was removed by tissue paper. The oil absorbing sample was then weighed. The equation q ($g.g^{-1}$) = (m_S - m_D)/m_D was applied to evaluate the oil absorbency, where m_D (g) was the weight of the dry sample and m_S (g) was the weight of the swollen sample.

3. Results and Discussion

Characterization of the magnetic composite

3.1. Attenuated Total Reflectance Fourier Transforms Infrared (ATR FT-IR)

Fig. 2 showed infrared spectra of the samples. In Fig. 2 (a), IR spectra of ATP, 3609cm^{-1} and 3459cm^{-1} peaks were assigned to (Al) O–H stretching vibration and the (Si) O–H stretching vibration of ATP respectively, and 1650cm^{-1} absorption peak was ascribed to –OH bending vibration [18]. These three characteristic peaks of ATP disappeared in the spectra of magnetic composite resin as shown in Fig. 2 (c). In the spectra of ATP–Fe_3O_4 as shown in Fig. 2 (b), the absorbance bands at 3404 cm^{-1} ascribed to the characteristic peak of –OH groups was very weak, suggesting that the crystallization was basically complete. In addition, the absorbance bands at 598 cm^{-1} and 461 cm^{-1} ascribed to the vibrations of Fe^{+2}─O^{2-} and Fe^{3+}─O^{2-}, were typical characteristics of spinel Fe_3O_4 [19]. It revealed that the materials contained crystallized spinel Fe_3O_4 and the nanoparticles absorbed onto ATP were Fe_3O_4. The absorption bands at 607 cm^{-1} and 487 cm^{-1} assigned to the Fe–O bond for spinel Fe_3O_4 particles in ATP-Fe_3O_4 [18] disappeared in the spectra of magnetic composite resin (figure 2 c). The characteristic band of Si–O–Si for ATP-Fe_3O_4 was observed around 1060 cm^{-1}. In Fig. 2 (c), the absorptions at 1223 and 1257 cm^{-1} were characteristic absorption peaks of MMA and absorptions at 923 and 966 cm^{-1} were butyl ester characteristic absorption peaks. Appearance of the peaks at 2937 cm^{-1} and 2865 cm^{-1} indicated the presence of saturated C–H stretching bands of both $–CH_3$ and $–CH_2$ groups. No peaks from 3000 to 3200cm^{-1} observed suggested all monomers had been polymerized. All of the results confirmed that the co-polymerization of MMA and BA on the surface ATP-Fe_3O_4 in the presence of APS has been initiated.

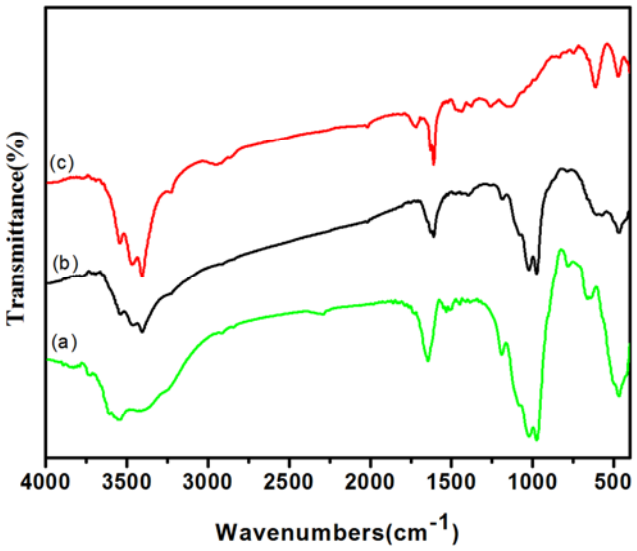

Fig. 2. *FT-IR of ATP (a), ATP-Fe_3O_4 (b) and magnetic composite resin (c).*

3.2. Thermogravimetric Analysis

Thermogravimetric analysis of the composite resin was used to evaluate the thermal stability of the Poly (MMA-BA)/ATP–Fe_3O_4 composites. Fig. 3 showed the first weight loss stage could be ascribed to the evaporation of water molecules, which were 5.38% and 4.36% for ATP-Fe_3O_4 and magnetic composite resin respectively [20]. Structure destroy of the composite resin started at 300oC, indicating that the composite resin had a higher thermostability. Compared with Poly (MMA-BA)/ATP–Fe_3O_4, ATP-Fe_3O_4 could not be almost decomposed at high temperatures, which showed little weight loss (8.10% below 600°C). So, the remaining mass for magnetic composite resin was attributed to the thermal resistance of ATP-Fe_3O_4 particles.

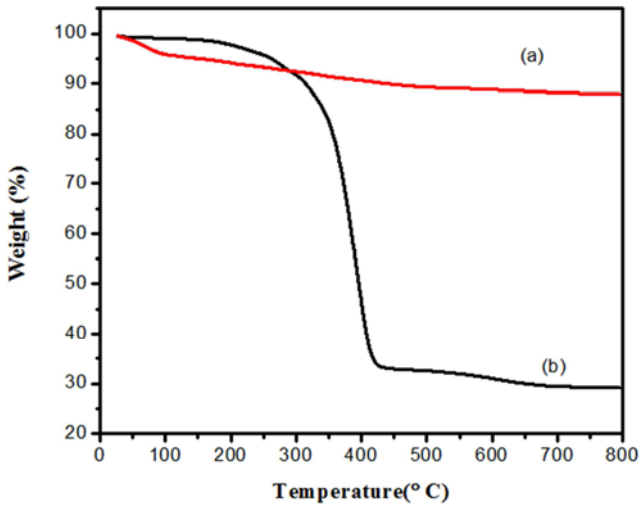

Fig. 3. *Thermogravimetric curves of ATP-Fe_3O_4 (a) and the magnetic composite resin (b).*

3.3. Scanning Electron Microscopy (SEM)

The morphologies of ATP, ATP-Fe_3O_4 and corresponding magnetic composite were observed by SEM. As shown in 4 A and 4 B, corresponding SEM images, also supported above conclusions. Due to the negative surface charges, iron cations could be bonded onto the surface of ATP via electrostatic forces easily [18] so that Fe_3O_4 particles obtained by co-precipitation process could disperse in situ onto the ATP surface. Fig. 4C displayed MMA-BA copolymer possessed a porous structure with a few of small pores. However, magnetic composite Poly (MMA-BA)/ATP-Fe_3O_4 containing modified ATP–Fe_3O_4 particles showed larger size pores and obviously different structure from MMA-BA copolymer (Fig. 4 D), which suggested that the incorporation of proper amount of ATP-Fe_3O_4 was benefit to improve the surface structure of the magnetic composite. Furthermore, the images also gave a direct observation that ATP-Fe_3O_4 was uniformly dispersed in the polymer matrix with good interface compatibility.

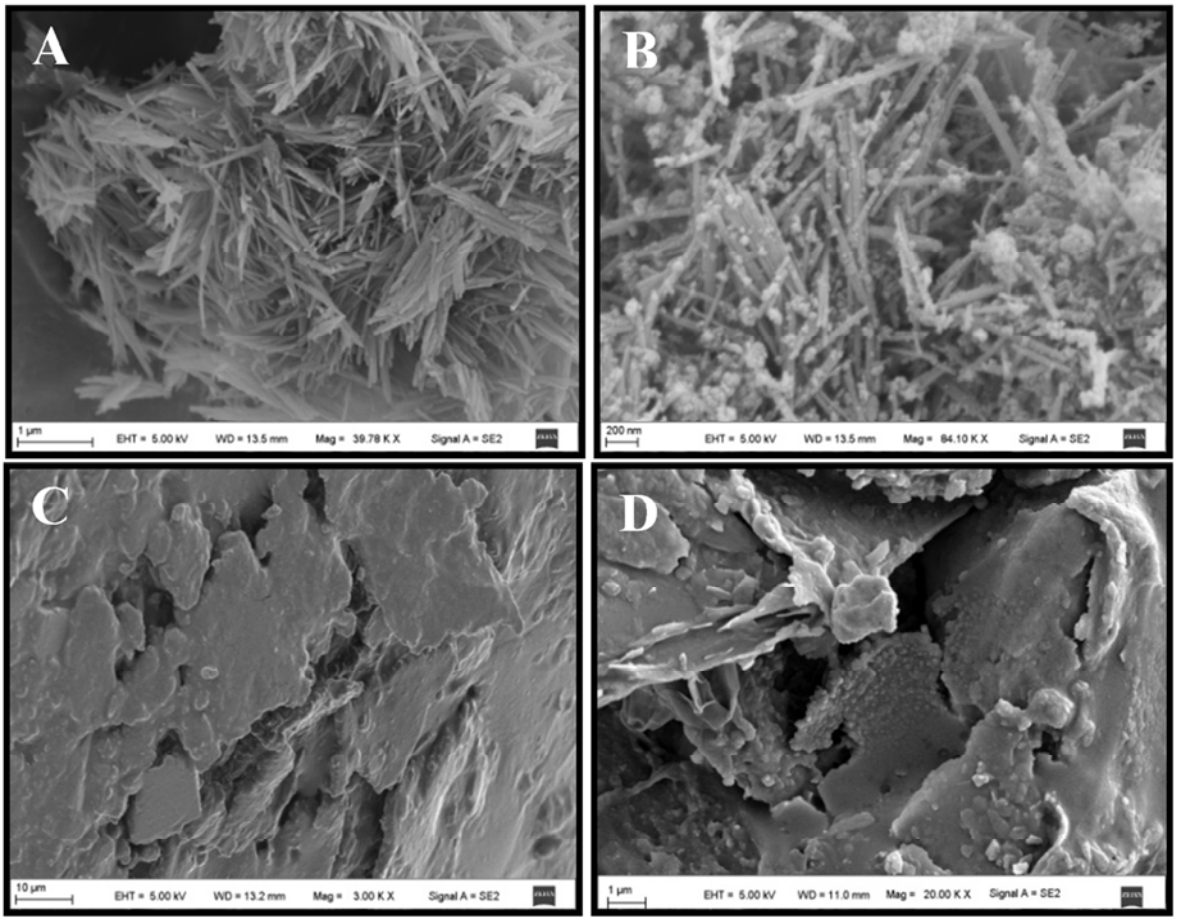

Fig. 4. *SEM images of ATP (A), ATP-Fe_3O_4 (B), MMA-BA copolymer (C) and poly (MMA-BBA)/ ATP–Fe_3O_4-(D).*

3.4. Transmission Electron Microscopy (TEM)

The morphologies of ATP, ATP-Fe_3O_4 and corresponding magnetic composite were observed by TEM. As shown in Fig. 5 (1), TEM image of ATP showed that ATP had a fibrillar single crystal structure, whose smallest structure unit possessed a length of 500–2000 nm and a diameter of 10–25 nm [21]. Fig. 5 (2) displayed that Fe_3O_4 nanoparticles uniformly dispersed on the surface of ATP fiber and the average thickness of raw ATP particles was 42 ± 8.0 nm, and the average size of Fe_3O_4 particles (black particles) was 10 nm.

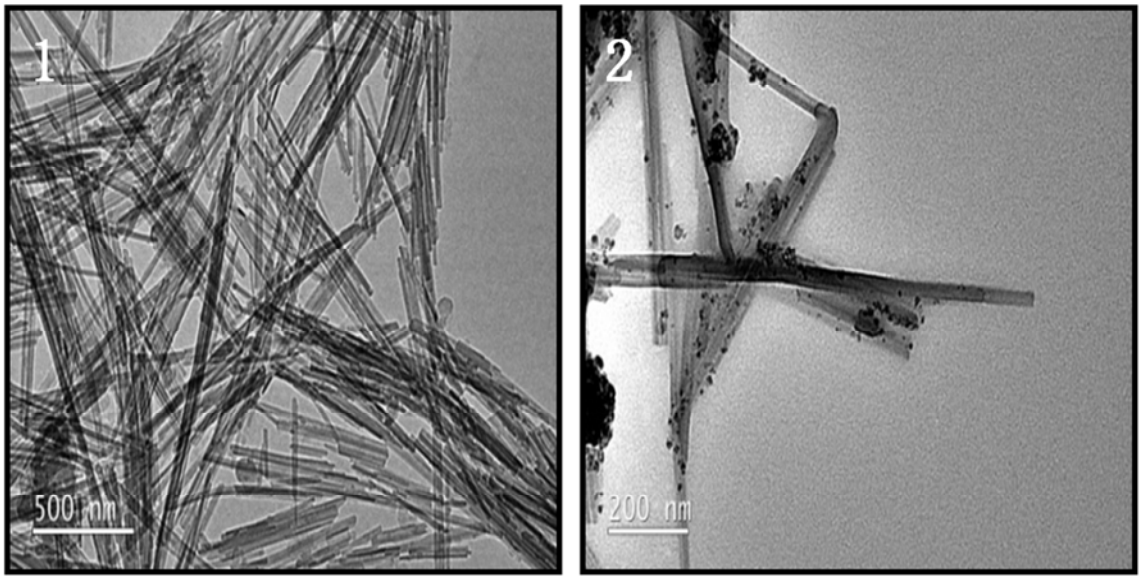

Fig. 5. *TEM images of ATP (1) and ATP-Fe_3O_4 (2).*

3.5. X-ray Diffraction (XRD)

Fig. 6 showed the X-ray diffraction (XRD) patterns of ATP-Fe_3O_4 (a) and magnetic composite resin (b). In the 2θ range of 20 – 70°, six characteristic peaks corresponding to Fe_3O_4 (2θ = 30.3°, 35.7°, 43.3°, 53.50°, 57.5°, and 63.0°) were observed in the ATP-Fe_3O_4 and magnetic composite resin, and the peaks could be indexed to (220), (311), (400), (422), (511) and (440) diffractions (JCPDS card (19-0629) for Fe_3O_4). In 27.01° appeared ATP (131) diffraction peak. The results suggested that the addition of raw ATP particles or polymers into Fe_3O_4 did not change its crystalline form. Moreover, it also could be seen that the XRD patterns of magnetic composite resin was similar to that of ATP-Fe_3O_4, indicating they had the same cylinder wall structure and interplanar spacing.

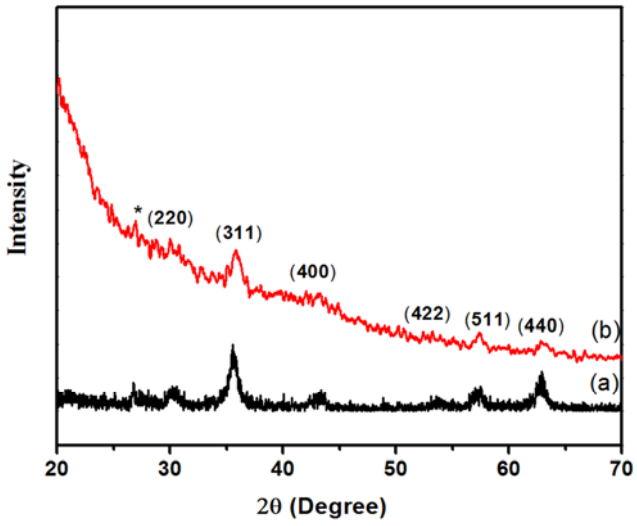

Fig. 6. *XRD patterns of (a) ATP-Fe_3O_4 and (b) magnetic composite resin.*

3.6. Magnetic Properties of the Modified ATP–Fe_3O_4 and Poly (MMA-BA)/ATP-Fe_3O_4 Magnetic Composite Resin

Fig. 7 showed the magnetic properties of the modified ATP–Fe_3O_4 and poly (MMA-BA)/ATP-Fe_3O_4 magnetic composite resin at room temperature. The saturation magnetization (Ms) value of the modified ATP–Fe_3O_4 was 0.481 emu.g^{-1}, while that of the magnetic composite resin was 0.132 emu.g^{-1}. It indicated that robust coating of MMA-BA on their surface and the introduction of the inorganic clay mineral of ATP quenched the magnetic moment of nanosized Fe_3O_4 particles by electron exchange between coating and surface atoms [22]. However, the magnetic composite resin still maintained an obvious magnetism, which was advantageous to separate the resin using a magnet.

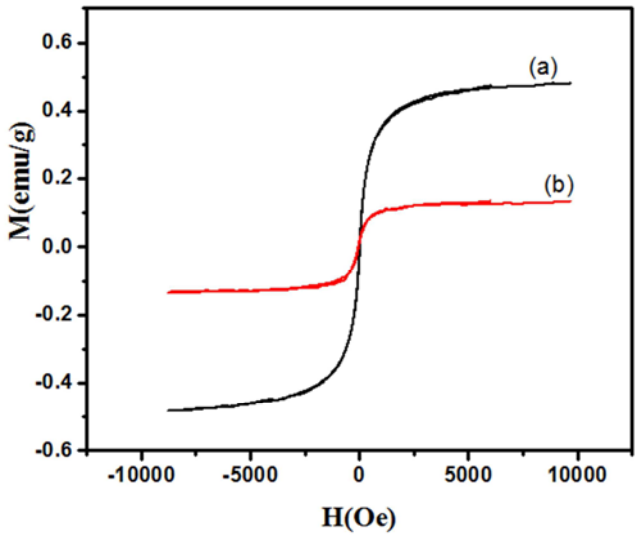

Fig. 7. *VSM measurement results of the ATP-Fe_3O_4 (a) and ATP–Fe_3O_4@ (MMA-BA) magnetic composite resin (b).*

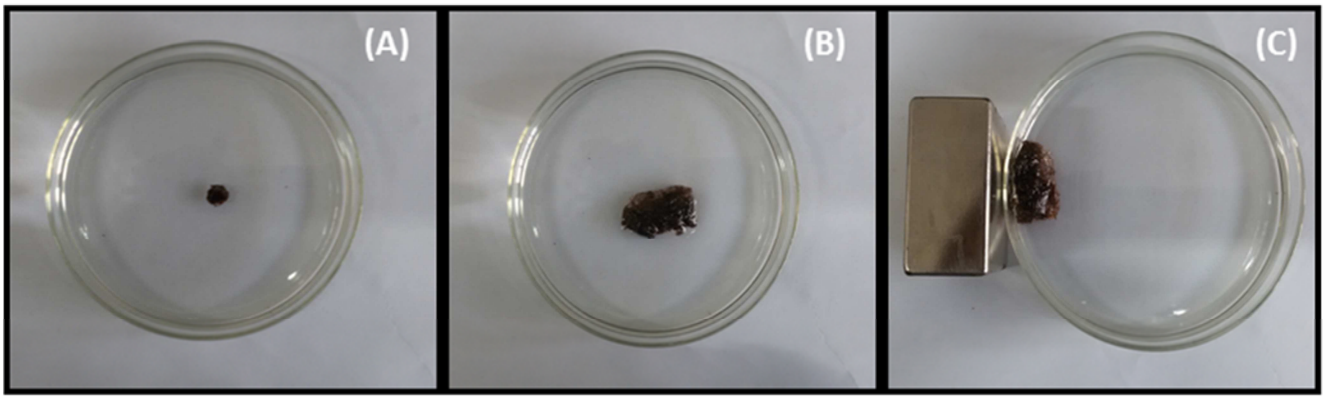

Fig. 8. *(A) - (C). Digital photograph images of oil absorbency from water surface of the magnetic composite resin under magnetic field.*

3.7. Digital Photograph Images of Oil Absorbency from Water Surface

As expected, the magnetism of the composite resin was related to its ability applied to environmental water treatment. The highly hydrophobic and superoleophilic nanoparticles exhibited a property called selective absorbance. Fig. 8 (A, B, C) was the digital photographs of oil absorbency from water surface by poly (MMA-BA)/ATP–Fe_3O_4 magnetic composite resin under magnetic field. Fig. 8 A - 8 B showed when it contacted with a layer of oil on a water surface, poly (MMA-BA)/ATP–Fe_3O_4 magnetic composite resin quickly absorbed the oil while repelling the water, then the oil-absorbed magnetic composite resin could be readily removed with a magnet bar over the water surface.

3.8. Optimization of Polymerization Conditions

3.8.1. Effect of Amount of Crosslinking

Effect of the amount of crosslinking on the oil absorbency was shown in Fig. 9 (a). Oil absorbency increased at first with increasing MBA concentration from 0.18 to 0.40 wt % and then decreased with further increase in MBA concentration. The oil absorbency reached the highest when the amount of crosslinking was 0.40%. If the amount of crosslinking was too small, resin density reduced and the ratio of soluble resin increased, so that the oil absorbency decreased. When the crosslinking content was below 0.25 wt %, the composite was semi-soluble and the oil absorbency could hardly be measured. As a result, the oil absorbency was very low, which was consistent with the Flory theory [23].

3.8.2. Effect of Amount of Initiator

Fig. 9 (b) showed the relation between the amount of initiator and the oil absorbency. The oil absorbency was the highest when the amount of initiator was 1.0%. It is known that the amount of initiator has important influence on molecular weight of polymer and effective network dimension of synthetic resin [24-28]. Where the oil absorbing resin was free of modified ATP–Fe_3O_4, the optimum amount of initiator was about 1.25%.

3.8.3. Effect of Monomer Ratio

The effect of monomer ratio on the crosslinking polymerization was investigated. Fig. 10 (a) an exhibited the relation between the monomer ratio and the oil absorption. It could be seen that the oil absorption curve showed a peak profile. With MMA content increasing, the oil absorption increased. Addition of MMA changed the stability of the network structure of the resins. However, if the amount of MMA was too great, the oil absorption reduced, because the lipophilicity was much worse than that of BA. Oil absorption reached its highest value of 22.07 g/g at the ration of MMA/BA of 1:1.

3.8.4. Effect of Amount of the Modified ATP–Fe_3O_4

The effect of the amount of the modified ATP- Fe_3O_4 on oil absorbency was shown in Fig. 10 (b). Oil absorption of the composite resin increased with the amount of the modified ATP- Fe_3O_4 increasing from 0.5 to 2.0 wt % and then decreased with further increase in the modified ATP-Fe_3O_4. The modified ATP–Fe_3O_4 occupied part of the interior space of the resin and was distributed in the resin dispersedly. When the amount of a modified ATP- Fe_3O_4 reached 2.0%; the oil absorption reached the highest of 25.0 g/g for toluene.

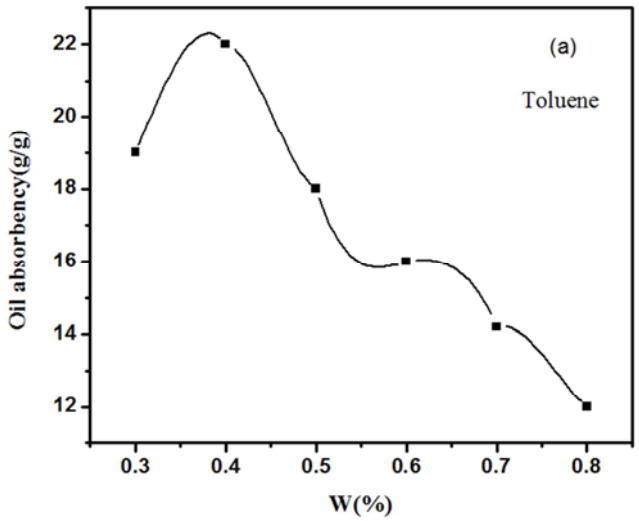

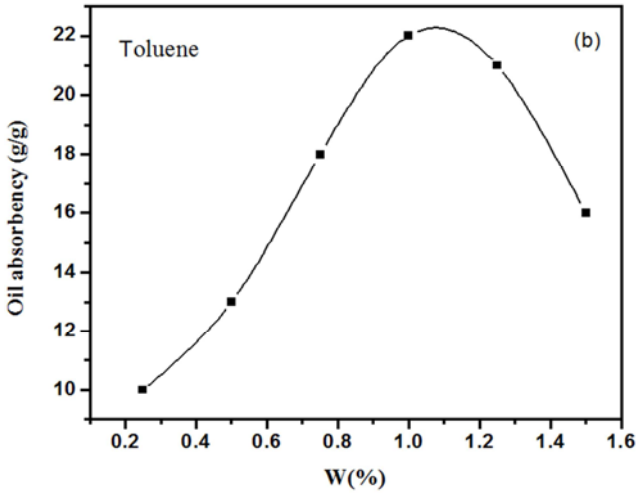

Fig. 9. (a) Relation between the amount of crosslinker and oil absorbency. (b) Relation between the amount of initiator and oil absorbency.

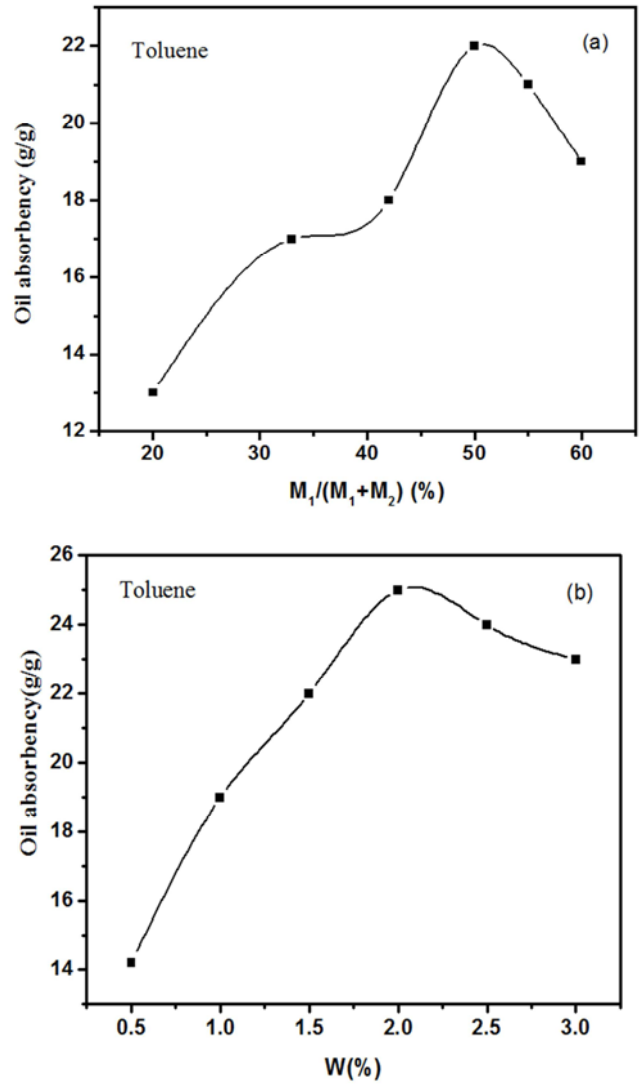

Fig. 10. (a) Relation between composition of monomer and oil absorbency. (b) The amount of the modified ATP- Fe_3O_4 on oil absorbency.

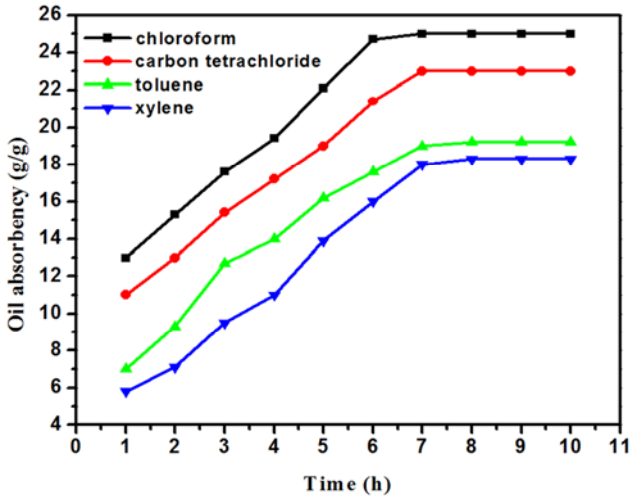

Fig. 11. Relation between oil absorbency and the absorption time.

3.9. Absorption Rate and Absorption Kinetics

To test the absorption rate, the sample was immersed in excess solvent at room temperature. And then it was taken out and weighed every 1 h. The absorption reached saturation after 7h the highest oil absorbency was respectively 18.3, 19.2, 23 and 25 g/g for xylene, toluene, carbon tetrachloride and chloroform. It could be seen from Fig. 11, oil absorbency increased rapidly at the beginning due to the solvation of the network chains. The main driving force of this process was the change in the free energies of mixing and elastic deformation. However, the swelling was limited, that is, with the time increasing the absorption rate became slower and finally reached saturation.

Absorption of oil onto the superabsorbent was studied in terms of the kinetics of the absorption mechanism by using three models. Assuming that the absorption kinetic process obeyed the first-order model, the kinetics equation was

$$\ln(q_e - q_t) = -k_1 t + A \quad (1)$$

Where q_t (g/g) was the amount of an absorption time t (h), k_1 was the rate constant of the equation (h^{-1}) and q_e was the amount of absorption equilibrium (g/g). The absorption rate constant k_1 could be determined experimentally by plotting of ln (q_e-q_t) versus t.

Similarly, if the absorption obeyed the second-order kinetics model, kinetics equation became following form:

$$\frac{1}{q_e - q_t} = k_2 t + B \quad (2)$$

Where k_2 (g/g.h) was the rate constant of the second order equation. The rate constant k_2 could be obtained by plotting 1/ (q_e-q_t) versus t.

The intraparticle mass transfer diffusion model was also one of useable kinetic models for describing a diffusion controlled kinetic absorption process [29, 30] is:

$$q_t = k_{id} t^{1/2} + C \quad (3)$$

Where K_{id} (g/g/$h^{1/2}$) was the rate constant of intraparticle diffusion, which could be measured by plotting qt verses $t^{1/2}$.

k_1, k_2 and k_{id} for the four kinds of oils, chloroform, carbon tetrachloride, toluene and xylene were respectively calculated from the slopes and listed in Table 1.1. Obviously the correlation coefficients for the first-order model were better than the second-order model, indicating that the first order model was more suitable to describe the absorption process. The correlation coefficients for the intraparticle diffusion model were over 0.9900 indicating that the absorption of these four oils onto the resin was mainly intraparticle diffusion controlled.

Corresponding linear fitting curves of the three models were showed in Fig. 12 (a, b, c).

Table 1.1. *Fitting results of the kinetic parameters.*

Oils	q_{max} (g/g)	The first-order model		The second-order model		Intraparticle diffusion model		
		k_1 (h^{-1})	R	k_2 (g/g.h)	R	Kid (g/g/$h^{1/2}$)	C (g/g)	R
Chloroform	32.6	0.2789	0.9957	0.03863	0.8921	7.810	4.549	0.9905
Carbon tetrachloride	30.0	0.2743	0.9930	0.03336	0.9557	7.398	2.900	0.9930
Toluene	25.0	0.3548	0.9939	0.04384	0.9337	7.463	-0.682	0.9970
Xylene	23.8	0.02674	0.9915	0.02535	0.9034	7.636	-3.088	0.9810

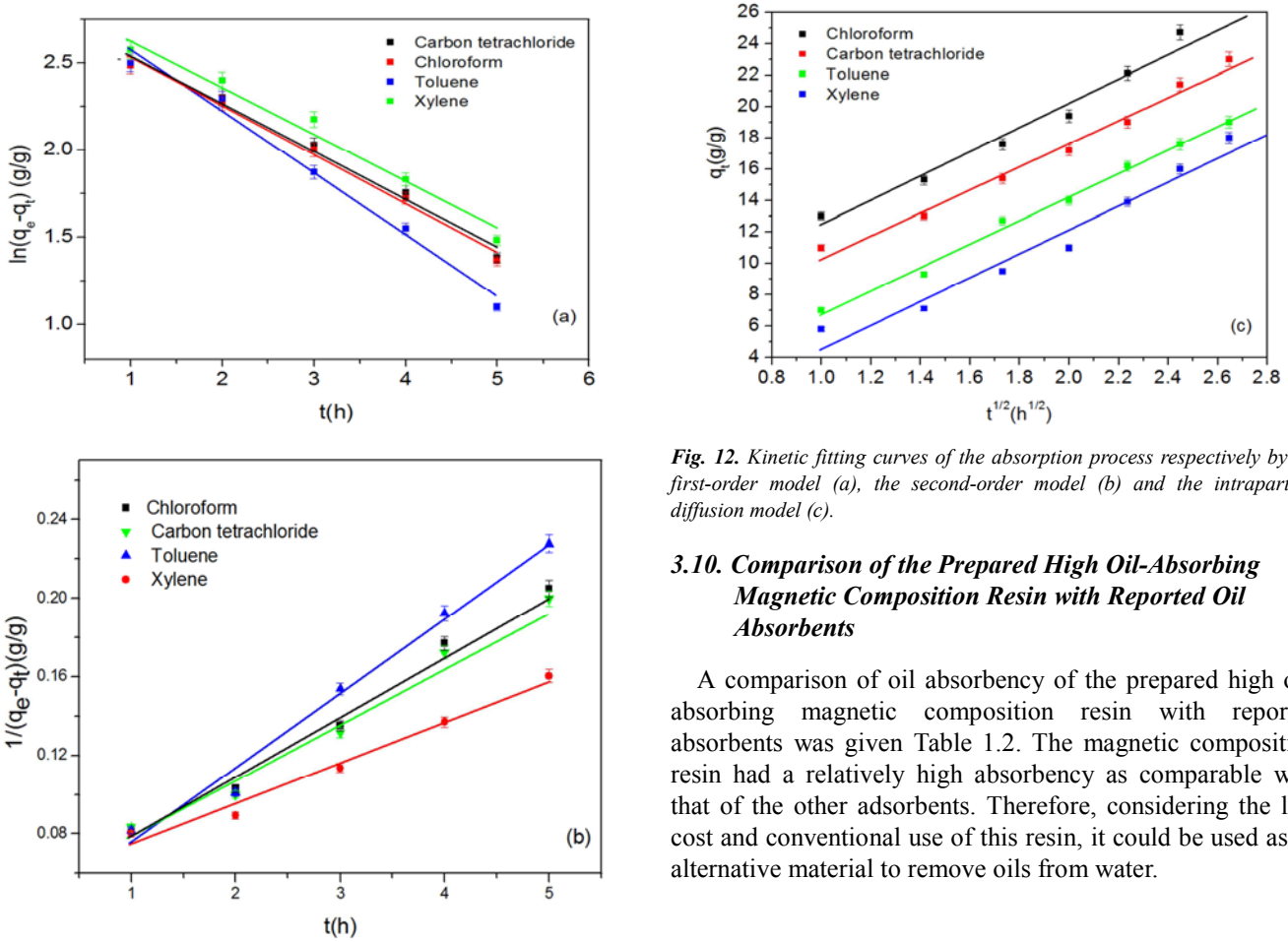

Fig. 12. *Kinetic fitting curves of the absorption process respectively by the first-order model (a), the second-order model (b) and the intraparticle diffusion model (c).*

3.10. Comparison of the Prepared High Oil-Absorbing Magnetic Composition Resin with Reported Oil Absorbents

A comparison of oil absorbency of the prepared high oil-absorbing magnetic composition resin with reported absorbents was given Table 1.2. The magnetic composition resin had a relatively high absorbency as comparable with that of the other adsorbents. Therefore, considering the low cost and conventional use of this resin, it could be used as an alternative material to remove oils from water.

Table 1.2. *Comparison of oil absorbency of the prepared high oil absorbing magnetic resin with reported oil absorbents.*

Oil absorbents	Oil absorbency (g/g)	References
Cetane methacrylate highly oil absorptive resin	36.6 for CCl_4	[31]
Oil absorption resin (B-PEHA)	30.88 for chloroform, 19.75 for toluene, 18.78 for xylene	[32]
CEMA/IOA copolymers	13.94 for toluene	[33]
Magnetic composite oil absorption resin	20 for chloroform, 10.5 for toluene	[34]
PC-CPMA	4.08 for toluene	[35]
Poly (Butyl Methacrylate-Styrene) highly oil absorptive resin	14.12 for toluene	[36]
poly (methyl methacrylate-butyl acrylate)/ATP–Fe_3O_4 magnetic composite	32.6 for chloroform, 30.0 for carbon tetrachloride, 25.0 for toluene, 23.8 for xylene	This work

4. Conclusion

A high oil-absorbing magnetic composite resin was synthesized by using a simple and conventional suspension polymerization method. It combined high oil-absorption with magnetic separation technology, because of its magnetic character; it can be easily collected by magnetic means in a short time. The prepared high oil absorption magnetic composite resin had higher oil absorbency than some previously reported oil absorptive materials, which indicated the prepared high oil absorption magnetic resin had a good application prospect. Kinetic investigation proved that the oil absorption obeyed the pseudo-first-order kinetic model and intraparticle diffusion model.

References

[1] Özen, İ., Şimşek, S., & Okyay, G. (2015). Manipulating surface wettability and oil absorbency of diatomite depending on processing and ambient conditions. Applied Surface Science, 332, 22-31.

[2] Chun C. L., Park J. W. Oil spill remediation using magnetic separation [J]. J. Environ. Eng., 2001, 127: 443-449.

[3] Zhou M. H., Cho W. J. Synthesis and properties of high oil-absorbent 4-tert-butylstyrene-EPDM-divinylbenzene graft terpolymer [J]. J. Appl. Polym. Sci., 2002, 85: 2119-2129.

[4] Zhou M. H., Hoang T., Kim I. G., Ha C. S., Cho W. J. Synthesis and properties of natural rubber modified with stearyl methacrylate and divinylbenzene by graft polymerization [J]. J. Appl. Polym. Sci. 2001, 79: 2464-2470.

[5] Martel, B., Morcellet, M. Sorption of aromatic compounds in water using polymer sorbents containing amino groups [J]. J. Appl. Polym., Sc., 1994, 51: 443-451.

[6] Chin, W. C., Orellana, M. V., Verdugo, P. Spontaneous assembly of marine dissolved organic matter into polymer gels. [J]. Nature, 1998, 391: 568-572.

[7] Galindo-Gonzalez C., de Vicente J., Ramos-Tejada M. M., Lopez-Lopez M. T., Gonzalez- Caballero F., Duran J. D. G., Preparation and sedimentation behaviorin magnetic fields of magnetite covered clay particles [J]. Langmuir, 2005, 21: 4410- 4419.

[8] Murray H. H., Transitional and new applications for kaolin, smectite, and palygorskite: a general overview [J]. Appl. Clay Sci., 2000, 17: 207-221.

[9] Sanchez C. M., Sanchez M. M., Factors influencing interactions of organo phosphorus pesticides with montmorillonite [J]. Geoderma, 19836, 29: 107-118.

[10] Ainsworth C. C., Zachara J. M., Ln Schimidt R. Quinoline sorption on Na-montmorillonite: contribution of the protonated a d neutral species [J]. Clay Miner., 1987, 35: 121-128.

[11] Rodriguez J. M., Lopez A. J., Bruque S. Interaction of Fenamiphos with montmorillonite [J]. Clay Miner., 1988, 36: 284-288.

[12] Shu H. T., Li D., Scala A. A., Ma Y. H., Adsorption of small organic pollutants from aqueous streams by alumina silicate-based micro-porous materials [J]. Sep. Purif. Technol., 1997, 11: 27-36.

[13] Torrents A., Jayasundera S. The sorption of non-ionic pesticides onto clays and influence of natural carbon [J]. Chemosphere, 1997, 35: 1549-1565.

[14] Danis T. G., Albanis T. A., Petrakis D., Pomonis P. J., Removal of chlorinated phenols from aqueous solutions by adsorption on alumina pillared clay sand mesoporous alumina aluminum phosphates [J]. Water Res., 1998, 32: 295-302.

[15] Konstantinou I. K., Albanis T. A., Petrakis D. E., Pomoni P. J. s, Removal of herbicides from aqueous solutions by adsorption on Al-pillared clays, Fe-Al pillared clays and mesoporous alumina aluminum phosphates [J]. Water Res., 2000, 34: 3123-3136.

[16] Huang D. J., Wang W. B., Xu J. X., Wang A. Q. A comparative adsorption study of β-naphthol on four polymeric adsorbents from aqueous solutions [J]. Chem. Eng. J., 2012, 210: 166-172.

[17] Mu B., Wang Q., Wang A. Q. Preparation of magnetic attapulgite nanocomposite for the adsorption of Ag+ and application for catalytic reduction of 4-nitrophenol [J]. J. Mater. Chem. A, 2013, 1, 7083-7090.

[18] Liu Y. S., Liu P., Su Z. X., Li F. S., Wen F. S., Attapulgite–Fe_3O_4 magnetic nanoparticles via co-precipitation technique [J]. Appl. Surf. Sci., 2008, 255: 2020–2025.

[19] Jiang L. P., Liu P. Design of magnetic attapulgite/fly ash/poly (acrylic acid) ternary nanocomposite hydrogels and performance evaluation as selective adsorbent for Pb 2+ion [J]. ACS Sustainable Chem. Eng., 2014, 2: 1785-1794.

[20] Liese H. C., Am. Miner., 1967, 52: 1198.

[21] Shen, L., Lin Y. J., Du Q. G., Zhong W., Yang Y. L., Preparation and rheology of polyamide-6/attapulgite nanocomposite and studies on their percolated structure [J]. Polymer, 2005, 46: 5758-5766.

[22] Mikhaylova M., Kim D. Y., Bobrysheva N., Osmolowsky M., Semenov V., Tsakalakos T., Muhammed M., Super para magnetism of magnetic nanoparticles: Dependence on surface modification [J]. Langmuir, 2004, 20: 2472-2477.

[23] Flory P. J. Principles of Polymer Chemistry, Cornell University Press: Ithaca, NY, 1953

[24] Atta A. M., El-Ghazawy R. A. M., Farag R. K., et al. Swelling and Network Parameters of Oil Sorbers Based on Alkyl Acrylate and Cinnamoyloxy Ethyl Methacrylate Copolymers [J]. J. Polym. Res., 2006, 13: 257-266.

[25] Atta A. M., El-Hamouly, S. H., Alsabagh, A. M., Gabr, M. M., Crosslinked poly (octadecene-alt-maleic anhydride) copolymers as crude oil sorbers [J]. J. Appl. Polym. Sci., 2007, 105: 2113-2020.

[26] Zhou X. M., Chuai C. Z. Synthesis and characterization of a novel high-oil-absorbing resin [J]. J. Appl. Polym. Sci., 2010, 115: 3321-3325.

[27] Wu B., Zhou M. H. Sorption of styrene from aqueous solutions with oil absorptive resin [J]. J. Environ. Manage, 2009, 90: 217-221.

[28] Atta A. M., El-Ghazawy R. A. M., Farag R. K. Crosslinked reactive macro monomers based on polyisobutylene and octadecyl acrylate copolymers as crude oil sorbers [J]. React. Funct. Polym, 2006, 66: 931-943.

[29] Weber Jr. W. J., Morris J. C., Removal of biologically resistant pollutants from waste waters by adsorption in Advances in Water Pollution Research. Pergamon Press Oxford, 1962. p. 231.

[30] Weber Jr. W. J., Morris J. C. Kinetics of absorption of oil onto the super absorbent from solution [J]. J. Sanitary Eng. Div. Am. Soc. Civ. Eng., 1963, 89: 31-60.

[31] Wang X. H., Synthesis of acrylic high-oil absorption resins, Edited by Deng X. C. and Dong X. F., Adv. Mater. Res., 2012, 502: 222-226.

[32] Yoo S. Y., Daud W. M. A. W., Lee M. G. Preparation of a biodegradable oil absorber and its biodegradation [J]. Bioprocess and biosystems engineering, 2012, 35: 283-288.

[33] Atta A. M, El-Ghazawy R. A. M, Farag R. K., El-Kafrawy A. F., Abdel-Azim A. A. A. Crosslinked cinnamoyloxyethyl methacrylate and isooctyl acrylate copolymers as oil sorbers [J]. "Polymer international 54.7 (2005): 1088-1096.

[34] Li P. X., Yu B., Wei X. C. Synthesis and characterization of a high oil-absorbing magnetic composite material [J]. J. Appl. Polym. Sci., 2004, 93: 894-900.

[35] Feng Y., Xiao C. F. Synthesis and properties of highly oil-absorptive resin with hydroxyl ethylacrylate as potential crosslinking agent [J]. Chin J. React. Polym. 2006, 15 (1): 45-49.

[36] Wu K., Chu X. Z., zou S. Y., Zhao Y. J., Xing W. H. Preparation of highly oil absorptive resin poly (butyl methacrylate-styrene) and its oil absorption performance [J]. J. Chem. Eng. Chin. Univ., 2013, 23 (1): 76-83.